

Physicochemical Properties of High-Molecular-Weight Plant Polysaccharide of Hexose Glycoside Class (Panavir) with Antiviral Activity

S. V. Stovbun^a, A. A. Berlin^a, A. I. Mikhailov^a, V. I. Sergienko^b, V. M. Govorun^b,
I. A. Demina^b, and T. S. Kalinina^c

^a *Semenov Institute of Chemical Physics, Russian Academy of Sciences, Kosygina ul. 4, Moscow, 119991 Russia*

^b *Research Institute of Physicochemical Medicine, Baltiiskaya ul. 8, Moscow, 119435 Russia*

^c *Zakusov Research Institute of Pharmacology, Russian Academy of Medical Sciences, Moscow, 125315 Russia*
e-mail: s.stovbun@chph.ras.ru

Received May 4, 2012; accepted May 16, 2012

Abstract—A high-molecular-weight plant polysaccharide belonging to the hexose glycoside (HG) class and composed of rhamnose (2–10%), arabinose (3–15%), glucose (10–67%), galactose (2–27%), xylose (0.1–3%), and mannose (0.1–5%) monosaccharides, as well as uronic acids (2–5%), had been isolated previously. It has high antiviral activity, as is proven by experimental models using hazardous and extremely dangerous viral infections such as herpes, cytomegalovirus, influenza, encephalitis, measles, rabies, and hepatitis C. The antiviral drug Panavir developed on its basis has an extremely low toxicity ($LD_{50} = 3000$) and is an antiviral and immunomodulatory agent. There has been no microscopic (instead of phenomenological) model of its biological or pharmacological activity because of a lack of knowledge about its physicochemical nature. In the present work, the results of a study on the physicochemical properties of the HG macromolecules which makes it possible to qualitatively explain the biological activity and pharmacological properties of Panavir are presented.

DOI: 10.1134/S1995078012050138

INTRODUCTION

A high-molecular-weight plant polysaccharide belonging to the hexose glycoside (HG) class and composed of rhamnose (2–10%), arabinose (3–15%), glucose (10–67%), galactose (2–27%), xylose (0.1–3%), and mannose (0.1–5%) monosaccharides, as well as uronic acids (2–5%), and having high antiviral activity, as was demonstrated by experimental models using hazardous and extremely dangerous virus infections such as herpes, cytomegalovirus, influenza, encephalitis, measles, rabies, and hepatitis C [1–6], has been previously isolated.

The antiviral drug Panavir developed on its basis has an extremely low toxicity ($LD_{50} = 3000$) and is an antiviral and immunomodulatory agent [7]. Technology for the preparation of Panavir substance is based on the use of peculiarities of polychromous kinetics of superslow molecular-dynamics processes (10^5 – 10^7 s), which are characteristic of physicochemical transformations in diffusion nonuniform media [8, 9].

Over 10 years of clinical practice, Panavir has shown high efficacy and safety when used in treating herpes, cytomegalovirus, human papilloma virus, influenza, tick-borne encephalitis, etc. [10]. Panavir is supplied as a solution for intravenous administration, as a suppository, and as a topical gel. In total, several

million patients have been treated with this drug over that period of time. However, there has been no microscopic (as opposed to phenomenological) model of its biological or pharmacological activity due to the lack of concepts concerning its physicochemical nature.

In the present work, results of a study on the physicochemical properties of the HG macromolecules which make it possible to qualitatively explain the biological activity and pharmacological properties of Panavir are presented.

MATERIALS AND METHODS OF INVESTIGATION

Panavir (manufactured by NIK LLC (the manufacturer's monograph number 42-0203-0657-06)) was used in this work. Physical and biochemical methods aimed at identifying lipids, glycolipids, proteins, peptides, sugars, and polysaccharides were used to investigate the molecular and chemical composition of the substance.

The lectrophoretic separation of the drug was carried out by one-dimensional electrophoresis under reducing conditions in a 9–16% gradient polyacrylamide gel (stacking gel contained 4% of acrylamide) with a length of 7 cm in a Tris-glycine Laemmli buffer followed by staining with Coomassie R250. The drug

Elemental analysis of Panavir

Phosphorus*	1322	Iron	48
Sulfur	122	Nickel	8
Chlorine	30	Copper	7
Potassium	391	Zinc	32
Calcium	248	Strontium	11
Manganese	6	Lead	6

* Elements per 1 vial (mg).

in an amount of 50 μg in 10 μL of Laemmli buffer containing 2% of sodium dodecylsulfate and 2.5% of dithiothreitol was kept at 95°C for 5 min. The electrophoresis was conducted under the following conditions: 10 mA in the stacking gel and 20 mA in the separating gel with cooling the chamber to 10°C.

A piece of gel with a diameter of 1.5 mm was washed in water for 15 min at room temperature. Then, 50 μL of a 1 : 1 (vol/vol) mixture of acetonitrile and 200 mM ammonium bicarbonate aqueous solution was added in a tube with the gel. Incubation was conducted at 50°C on a shaker for 45–60 min. The solution was collected and acetonitrile (50 μL) was added to dehydrate the gel. Incubation was conducted at room temperature for 20 min. Acetonitrile was thoroughly collected. Thereafter, 20 μL of trypsin working solution (5 μL of the original trypsin solution (Agilent, United States), 25 μL of water, and 10 μL of 200 mM ammonium bicarbonate aqueous solution) was added to the tube. To conduct the cleavage reaction, the tube with gel was transferred to a thermostat with a temperature of 37°C and incubated for 12 h. To extract the peptides, 5 μL of a freshly prepared 0.1–0.5% (vol/vol) solution of trifluoroacetic acid (TFA) in water was added to the tube.

To perform the mass spectrometric analysis, 2 μL of the sample solution and 0.3 μL of 2,5-dihydroxybenzoic acid solution (20 mg/mL in 20% aqueous acetonitrile with 0.5% of trifluoroacetic acid) were mixed on a ground steel substrate. Mass spectra were obtained on an Ultraflex II (Bruker Daltonics) tandem MALDI time-of-flight mass spectrometer equipped with a UV laser (Nd) in the positive ion reflection mode. To identify carbohydrates and peptides contained in the drug, the sample was studied using a chromatography–mass spectrometry system composed of an Ultimate 3000 (Dionex, United States) chromatograph and a Maxis ESI-QUAD-TOF mass spectrometer (Bruker Daltonics, Germany). Elemental analysis was conducted on a S2 PICOFOX spectrometer (Bruker AXS, Germany).

An acoustical ultrasonic spectral analysis of macromolecule size was carried out using a PA Fast Sizer 100 instrument (Partikel-Analytik-Messgeräte, Germany) at an aqueous solution concentration of 2% and at a temperature of 21°C. The measurement method is

based on attenuating a high-frequency (1–100 MHz) ultrasonic wave being passed through the sample. Since the attenuation spectrum depends on the particle-size distribution function, the apparatus function makes it possible to construct a particle-size distribution function wherein no additional assumption about the character of the function itself is required for this purpose.

A determination of the particle size by the dynamic light-scattering method was carried out on a 90Plus particle-size analyzer (Brookhaven Instruments Corporation, United States).

Electron microscopy of the particles precipitated from the HG aqueous solutions with different concentrations was performed on a silicon substrate by means of a LEO SUPRA 25 scanning field-emission electron microscope (Zeiss, Germany).

Circular dichroism (CD) spectra were obtained on a SKD-2 spectrometer (Institute of Spectroscopy, Russian Academy of Sciences), and the rotation angle of the plane of polarization of solutions, φ , was measured on a Palomat-A polarimeter.

RESULTS AND DISCUSSION

The HG solutions are optically active because sugar residues, from which the macromolecules are built up, are homochiral. At the same time, circular dichroism spectra are not observable under these conditions.

The chemical diversity of functional groups and molecules includes the above-listed monosaccharides and uronic acids, as well as various unidentifiable peptides and proteins found in the course of the study (about 100 various tryptic peptides, peptide nontryptic fragments (Fig. 1), as well as the RuBiSco protein, small and large subunits, being the major fraction of plant cells), which are present in substantially lower amounts (overall, less than 1%) and traces of lipids. Glycyrrhizic acid was detected in trace amounts in the course of an analysis of saponins. An elemental analysis revealed a relatively large phosphorus content of about 1%, which is five times higher than calcium and potassium concentrations and one order of magnitude (or even more) higher than concentrations of other elements (manganese, iron, nickel, copper, zinc, etc.) (see the table).

The unimodal size distribution of HG nanoparticles with an average value of $D = 140$ nm and dispersion of 100 nm was obtained by the acoustical ultrasonic spectral analysis method (because this method does not require additional information about the character of the distribution function). The average value of the diameter of nanoparticles obtained by the dynamic light-scattering method for the studied concentration range (1–10%) is practically constant for a monomodal distribution function and is equal to $D = 350$ nm, with the value of dispersion being equal to 200 nm. It is probable that the closeness of the diame-

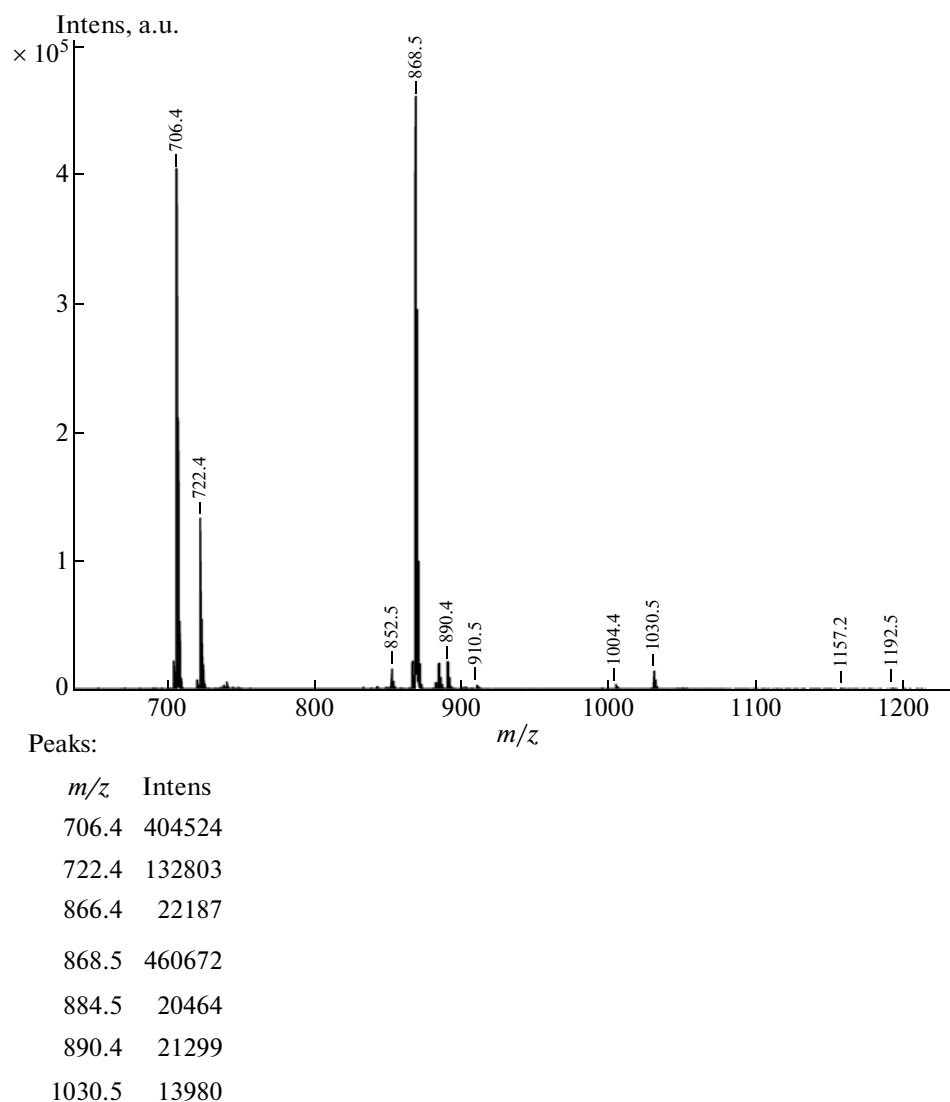


Fig. 1. Direct mass spectrometric analysis of Panavir.

ter values over a wide range of concentrations may give evidence of a slight deformability of nanoparticles in the solution, as well as of the absence of the processes of any efficient aggregation of these particles.

Results of the electron microscopy of the HG macromolecules precipitated on the silicon substrate from the solution with a concentration of 0.01% are presented in Fig. 2. An estimation of the average diameter of HG nanoparticles gives a value of $D = 250$ nm with a dispersion of 150 nm.

The data on the diameters of nanoparticles obtained experimentally by the three independent methods correspond well to each other; this confirms the reliability of these results. Note that the lowest out of the three diameter values was obtained when the ultrasound attenuation factor was measured. This is probably due to the radial localization of the nanoparticle mass effective for the dissipation of the ultra-

sound energy. The highest average diameter value obtained by the dynamic light-scattering method corresponds most likely to the region of the diffusively distributed nanoparticle substance with the sufficient value of the optical density when compared to the solvent (water). Upon water drying, nanoparticle compaction occurs, which is indeed confirmed by a decrease in the average diameter of HG particles to a value of 250 nm obtained by the electron microscopy of the solution that precipitated on the silicon substrate. Since short-range interaction effects are the most important ones in biological systems, the highest of the three values, namely $D = 350$ nm, will be hereinafter taken conventionally as an effective radius of the Panavir nanoparticles.

Note also that the closeness of the values of the nanoparticle diameters measured in the solution (at different concentrations and by using rather different

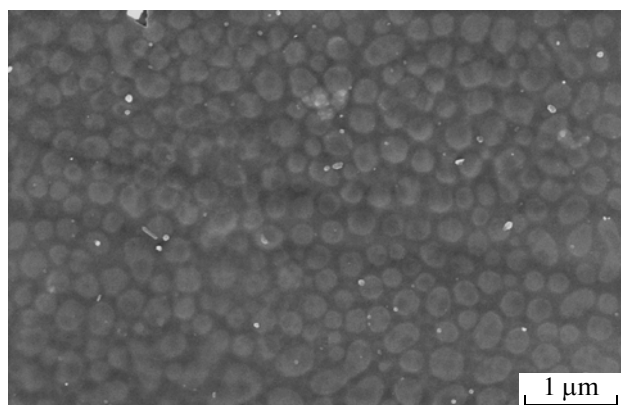


Fig. 2. Electron microphotograph of Panavir nanoparticles precipitated onto a silicon substrate.

methods) and upon precipitation on the substrate and drying of the solution, i.e., under conditions of water removal from the inner volume of the particle, most likely indicate that the nanoparticle is stable and composed of strongly bound associates of HG macromolecules.

The above results of the measurement of Panavir nanoparticle diameters also agree with a simple experimental observation of the absence of the Tyndall effect in the solution of HG, which means the fulfillment of the $D \sim \lambda$ relation, where λ is the light wavelength ($\lambda = 400$ nm).

The experimentally determined value of the HG solubility limit at the temperature of 36.6°C and $\text{pH} = 7$ turned out to be equal to $C^* = 11.4\%$ (the solubility factor is 0.13), with the substance characteristic dissolution times being equal to tens of seconds or to minutes under conditions of stirring with a cyclic frequency of about 1 Hz.

The Stokes viscosity of the aqueous solutions changes slightly at these concentrations and practically does not depend on the temperature ($20\text{--}40^\circ$); it roughly corresponds to the water viscosity.

The above value of the saturated solution concentration, $C^* = 11.4\%$, and the fact that the solution does not have viscoelastic properties up to the concentration of monomers (monosaccharides) close to the percolation threshold [11] unambiguously indicate that the solution is composed of weakly interacting (practically without engagements) clusters (of monomers). Indeed, near the percolation threshold, the correlation radius converges quickly to infinity in the case of interacting clusters, whereupon the solution viscosity would have substantially increased as well [11]. These data may be explained only by the presence of a charge on the nanoparticles, which is indeed confirmed by the results of the measurement of the zeta potential and the mobility of nanoparticles in the electric field. Indeed, the measured average values of the zeta potential, $Z = -26.7$ mV, and of mobility, $f = -2.1$ μs , for the HG concentration of 0.5%, and

-25.1 mV and -1.96 μs for the concentration of 1.0%, respectively, indicate that the particles have an uncompensated negative charge, probably determined by the negatively charged sugar residues. It is obvious that the repulsion of nanoparticles is associated with their surface charge, since the scale of efficacious shielding of the Coulomb repulsion in water is, for example, for proteins lower than 0.5 nm [12]. In fact, this means that the Coulomb interaction is shielded in the first two solvation shells formed by the charged functional groups.

One may assume that the complete filling of the physical volume of the solvent with the spherical particles' own volume, which may be neglected (because the liquid level remains practically unchanged in this case), is a condition for the formation of the condensed phase of nanoparticles in the form of a film on the solution surface at the C^* value.

Therefore, the HG solution consists of negatively charged clusters with a size of 350 nm partially separated by polarized layers of water molecules which ensure the mutual sliding of the nanoparticles and a viscosity close to that of water up to concentrations of the saturated solution.

It is known that the linear starch fraction (amylose) is colored in iodine solutions as a result of the formation of a guest–host structure. In this case the very macromolecule is assembled into a spiral-like shape, whereas the cross-linked three-dimensional starch fraction (amylopectin) does not become colored at all [13]. The insignificance of this effect for the HG solutions may indicate the presence of a sufficiently strong intermolecular (monomeric) interaction inside the nanoparticle, resulting in its structurelessness.

The absence of circular dichroism effects for the solutions of the HG nanoparticles also confirms the assumption about the structurelessness of their internal space. Indeed, the circular dichroism effect is observed in the aqueous nanocellulose solutions because of a high degree of complementarity of glucopyranose rings ensured by the short-range hydrogen bonds and by the formation of spiral-like structures [14].

Contrariwise, as our measurements indicate, the circular dichroism effects in the case of trinitrocellulose, wherein there is an almost complete substitution of OH–groups (ensuring the complementarity of glucopyranose rings) by NO_2 groups and, correspondingly, a weakening of the intermolecular interaction and a homogenization of the internal space of the nitrocellulose macromolecule occur, are not observed at all.

The internal space of the HG nanoparticle is most likely a strongly bound (by physical and chemical bonds) three-dimensional structureless (isotropic and homogeneous) molecular lattice with a previously established molecular composition. The resilience or low deformability of the nanoparticle is enhanced by the Coulomb interaction of the charged functional groups located inside the space.

The existence of such chemical groups and molecules, both similarly charged ones and those having polyelectrolyte properties, is confirmed by the chemical diversity of the substance composition as established in the present work. In this case the presence of a noticeable amount of peptides, as well as of phosphorus (about 1%), may result in the formation of an electrically neutral (polyelectrolyte) structureless nanoparticle core (previously detected when measuring the ultrasound attenuation) where the effective mass of the particle is concentrated.

Note that the concept about the hydrophobic interactions resulting in the compaction of the nanoparticle seems less likely if one simply takes into account the chemical composition and diversity ascertained for it, i.e., a substantially higher amount of hydrophilic molecular domains and, correspondingly, low or trace amounts of lipids. Therefore, physicochemical properties of the HG solutions may be explained by the existence of three-dimensionally bound nanoparticles with a size of 350 nm.

The internal space of the nanoparticles is structureless; they have a molecular weight $M = 10^8 - 10^9$ Da and an uncompensated negative charge and weakly interact and do not aggregate with each other up to the saturated solution concentrations. At the same time, in spite of having a wide diversity of unidentifiable biochemical fragments, peptides, proteins and functional groups, the Panavir nanoparticles are visualized as almost regular spheres of about the same diameter and the developed industrial nanotechnology for the preparation of monodisperse Panavir particles revealing pharmacological activity is distinguished by high reproducibility and meets the standards of the Ministry of Health of the Russian Federation.

In conclusion, a simple biophysical model of Panavir that is sufficient to qualitatively explain the action of this drug may be formulated as follows.

One therapeutic dose contains nanoparticles in an amount of $10^{10} - 10^{11}$. This value corresponds to and even substantially exceeds the amount of viral particles in the body at the prelethal stage.

Being similar to a virus and having a significant charge on the surface, polysaccharide particles induce a considerable stimulation of various components of the immune response, the fact of which was demonstrated by conducting medicinal trials using pharmacological preparation. Analogues which have similar mechanisms of immunity stimulation are known [15, 16]; however, the stability of HG makes us assume that it is the most active component. Its physicochemical properties make it possible to achieve therapeutic effects without any of the adverse events recorded for analogous immune-response stimulators.

REFERENCES

1. S. V. Stovbun, A. A. Litvin, P. V. Yakimuk, and V. I. Sergienko, RF Patent No. 2335289, Byull. Izobret., No. 28 (2008).
2. S. V. Stovbun, A. V. Lepekhin, L. I. Ratnikova, A. A. Litvin, V. I. Sergienko, "Experience of Use of Panavir in Therapy of Tick-Borne Encephalitis," *Infekts. Bolezni* **5** (1), 41–46 (2007).
3. S. V. Stovbun, T. S. Kalinina, L. N. Nerobkova, T. A. Voronina, A. A. Litvin, and V. I. Sergienko, "Study of Antiparkinsonic Activity of Panavir on a Model of Parkinson Syndrome Induced by Systemic Administration of MPTP to Outbred Rats and C57BL/6 Mice," *Bull. Exp. Biol. Med.*, **140**, 55–57 (2005).
4. S. V. Stovbun, P. G. Deryabin, A. A. Litvin, and V. I. Sergienko, "Action of Panavir on Experimental Infection Caused by Hepatitis C Virus in Cell Cultures," *Infekts. Peredav. Polovym Putem*, No. 3, 31–33 (2003).
5. S. V. Stovbun, S. V. Gribencha, A. A. Litvin, M. A. Kokhnovich, V. I. Sergienko, P. V. Yakimuk, and V. G. Bezmen, "Defense Activity of Panavir Preparation at Experimental Rabic Infection," *Antibiot. Khimioter.* **54** (5–6), 31–36 (2009).
6. S. V. Stovbun, E. N. Prokudina, G. A. Galegov, N. P. Semenova, T. A. Grigor'eva, T. S. Kalinina, A. A. Litvin, and V. I. Sergienko, "Effect of Panavir Preparation on Reproduction of Influenza Virus," *Antibiot. Khimioter.* **51** (6), 7–10 (2006).
7. S. V. Stovbun, L. V. Kolbukhina, N. N. Nosik, L. N. Merkulova, D. M. Braginskii, L. A. Lavrukhina, T. S. Kalinina, A. A. Litvin, and V. I. Sergienko, "Time Course of Leukocyte Interferon Induction after Single and Repeated Application of Panavir," *Tsitokiny Vospaleniya*, **8** (2), 49–52 (2009).
8. T. P. Shcherbakova, V. A. Demin, and A. I. Mikhailov, "Polychronous Kinetics of Oxidative Delignification of Coniferous Kraft Cellulose with Hydrogen Peroxide," *Russ. J. Appl. Chem.* **77**, 1725–1729 (2004).
9. S. V. Stovbun and A. I. Mikhailov, in *Proceedings of the XXIII Symposium Modern Chemical Physics, Tuapse, Russia, 2011*, p. 123.
10. S. V. Stovbun, V. I. Sergienko, V. I. Kulakov, N. M. Podzolkova, A. A. Litvin, et al., *Panavir: Experience of Use in Clinical Practice – Gynecology* (Nauchn.-Issl. Inst. Fiz.-Khim. Med. Ross. Akad. Med. Nauk, Moscow, 2007) [in Russian].
11. P. G. De Gennes, *Scaling Concepts in Polymer Physics* (Cornell Univ., Ithaca, 1979; Mir, Moscow, 1982).
12. V. S. Sivozhelezov, Extended Abstract of Doctoral Dissertation in Biology (Inst. Biofiz. Kletki Ross. Akad. Nauk, Moscow, 2002).
13. V. P. Kotov and V. N. Shvedova, *Biochemistry* (Drofa, Moscow, 2006) [in Russian].
14. R. Witter, U. Stenberg, S. Hesse, T. Kondo, F.-T. Koch, and A. Ulrich, "¹³C Chemical Shift Constrained Crystal Structure Refinement of Cellulose Ia and Its Verification by NMR Anisotropy Experiments," *Micromolecules* **39**, 6125 (2006).
15. A. E. Nel, L. Madler, D. Velegol, T. Xia, E. M. V. Hoek, P. Somasundaran, F. Klaessig, V. Castranova, and M. Thompson, "Understanding Biophysicochemical Interactions at the Nano-Bio Interface," *Nat. Mater.* **8**, 543–557 (2009).
16. M. Auffan, J. Rose, J.-Y. Bottero, G. V. Lowry, J.-P. Jolivet, and M. R. Wiesner, "Towards a Definition of Inorganic Nanoparticles from an Environmental, Health and Safety Perspective," *Nat. Nanotechnol.* **4**, 634–641 (2009).